NIH Public Access
Author Manuscript
Dev Dyn. Author manuscript; available in PMC 2013 December 01.

Published in final edited form as:
Dev Dyn. 2012 December ; 241(12): 2005–2013. doi:10.1002/dvdy.23886.

Distinct expression patterns of *Sulf1* and *Hs6st1* spatially regulate heparan sulfate sulfation during prostate development

Rita A. Buresh-Stiemke[a], **Rita L. Malinowski**[a], **Kimberly P. Keil**[b], **Chad M. Vezina**[b], **Arie Oosterhof**[c], **Toin H. van Kuppevelt**[c], and **Paul C. Marker**[a,†]

[a]Division of Pharmaceutical Sciences, School of Pharmacy, University of Wisconsin – Madison, 777 Highland Ave., Madison, WI, USA [b]Department of Comparative Biosciences, School of Veterinary Medicine, University of Wisconsin – Madison, 1656 Linden Dr., Madison, WI USA [c]Department of Biochemistry 194, Radboud University Nijmegen Medical Center, NCMLS, P.O. Box 9101, 6500 HB Nijmegen, The Netherlands

Abstract

Background—Prostate morphogenesis initiates in the urogenital sinus (UGS) with epithelial bud development. Sulfatase-1 (SULF1) inhibits bud development by reducing extracellular heparan sulfate (HS) 6-*O* sulfation and impairing FGF10 signaling via the ERK1/2 mitogen activated kinases.

Results—We characterized the expression patterns of HS 6-*O* sulfation modifying enzymes in the developing prostate by *in situ* hybridization and showed that *Sulf1* and *Hs6st1* had overlapping but distinct expression domains. Notably, *Hs6st1* was present while *Sulf1* was excluded from the tips of elongating epithelial buds. This predicted relatively high HS 6-*O* sulfation at the tips of elongating epithelial buds that was confirmed by immunohistochemistry. The pattern of *Sulf1* expression in the peri-mesenchymal epithelium matched predicted locations of BMP signaling. Exogenous BMP4 and BMP7 induced *Sulf1* expression in the UGS, decreased epithelial HS 6-*O* sulfation, and reduced ERK1/2 activation in response to FGF10.

Conclusions—These data suggest that BMPs limit FGF10 action in the developing prostate at least in part by inducing *Sulf1.*

Keywords

SULF1; extracellular sulfatase 1; HS6ST1; BMP4; BMP7; FGF10; prostate development; ductal morphogenesis

Introduction

The prostate is a male-specific exosecretory gland that develops from the urogenital sinus (UGS) in response to androgens during late embryonic development. Paracrine interactions between the urogenital sinus mesenchyme (UGM) and the urogenital sinus epithelium (UGE) are required for prostate development (Marker et al., 2003). Some paracrine growth factor pathways have been shown to promote growth and/or branching morphogenesis during prostate development while other paracrine pathways inhibit growth and/or branching morphogenesis (Prins and Putz, 2008).

[†]Address all correspondence and requests for reprints to: Paul C. Marker, Division of Pharmaceutical Sciences, School of Pharmacy, University of Wisconsin, 777 Highland Ave, Madison, Wisconsin, 53705, USA, marker@wisc.edu, 608-890-2150 (voice), 608-262-5345 (FAX).

NIH-PA Author Manuscript
NIH-PA Author Manuscript
NIH-PA Author Manuscript

NIH-PA Author Manuscript

NIH-PA Author Manuscript

NIH-PA Author Manuscript

Normal prostate development occurs through the coordinated actions of these paracrine pathways that are determined, in part, by the spatially and temporally regulated expression patterns of growth factors, receptors, and other signaling pathway components. Epithelial growth and branching are promoted by fibroblast growth factor-10 (FGF10)(Huang et al., 2005). *Fgf10* is expressed in regions of the UGM known as the mesenchymal pads that are located adjacent to the epithelial bud forming domains. FGF10 promotes epithelial duct outgrowth by binding the epithelial specific isoform of fibroblast growth factor receptor-2-IIIb (FGFR2IIIb) and subsequently activating mitogen activated protein kinase (MAPK) signaling (Thomson and Cunha, 1999; Kuslak and Marker, 2007). FGF10-null ($Fgf10^{-/-}$) UGSs fail to develop into prostates in the presence of active androgen signaling (Donjacour et al., 2003). Furthermore, conditional loss of FGFR and the FGFR substrate-2α in the developing mouse prostate impaired branching morphogenesis (Zhang et al., 2008; Lin et al., 2007). Thus, the FGF10 signaling pathway has been identified as necessary for prostate development. Epithelial growth and branching are inhibited by bone morphogenetic proteins (BMPs) including BMP4 and BMP7. *Bmp4* localizes to the lamina propria [also known as the peri-epithelial mesenchyme (Abler et al., 2011a)] of the E17 and P1 UGS and is also localized to the mesenchyme separating epithelial bud outgrowths (Prins et al., 2006; Lamm et al., 2001). Exogenous BMP4 impaired testosterone-induced prostate ductal budding and epithelial proliferation in cultured UGS tissues. Similarly, *Bmp7* localizes to the lamina propria adjacent to the most proximal portion of prostatic buds on E17 but is not present in the mesenchyme near the tips of invaginating epithelial buds. As ductal morphogenesis progresses to branching morphogenesis, *Bmp7* expression is induced in the epithelium of the bud tips (Grishina et al., 2005; Huang et al., 2005). Exogenous BMP7 impaired UGS bud development in cultured UGS tissues by reducing the number of NOTCH1 signaling domains and has overlapping function with BMP4 (Grishina et al., 2005). Furthermore, the endogenous BMP4 and BMP7 antagonist, Noggin, promotes P63-positive cell proliferation in the epithelial bud tips further contributing to functional patterning of growth factors and growth factor modulators in UGS development (Cook et al., 2007). Knockout mice containing null alleles for either *Bmp4* ($Bmp4^{+/-}$) or *Bmp7* ($Bmp7^{lacz/lacz}$) also have increased branching morphogenesis of the prostate further confirming their inhibitory roles during prostate development (Lamm et al., 2001; Grishina et al., 2005).

Heparan sulfate (HS) can modulate paracrine growth factor signaling either by binding growth factors and impairing the interaction with their cognate receptors or by facilitating ligand-receptor complexes to activate signaling pathways. HS is the polysaccharide component of heparan sulfate proteoglycans, which make up part of the extracellular matrix. HS is comprised of disaccharide repeats that contain glucosamine and uronic acid monomers. These disaccharides are modified by sulfation at the *N*-, 3-*O* and 6-*O* moieties of glucosamine and the 2-*O* moiety of uronic acid (Esko and Lindahl, 2001). The specific sulfation patterns on the HS polysaccharide contribute to the regulation and patterning of paracrine growth factor signaling pathways. The interaction of HS with FGF10-FGFR2IIIb in a ternary complex promotes signaling and is specifically facilitated by 6-*O* sulfation of glucosamine (Yeh et al., 2003). In contrast, 6-*O* sulfated HS can bind to Noggin extracellularly which further impairs BMP4 signaling *in vitro* (Viviano et al., 2004).

Three heparan sulfate 6-O sulfotransferases (HS6ST-1, -2, and -3, as well as one alternatively spliced form HS6ST-2S) introduce 6-*O* sulfation on specific HS disaccharide sequences during intracellular synthesis (Habuchi et al., 2003; Habuchi et al., 2000). These enzymes have functional redundancy but favor the addition of sulfates to an uronic acid residue neighboring the *N*-sulfoglucosamine. The expression patterns of the three HS6ST enzymes overlap but are distinct during vertebrate development (Zhao et al., 2006; Ratzka et al., 2010), but *Hs6st1* knockout mice ($HS6ST1^{-/-}$) have the most significant phenotype with late embryonic lethality (Habuchi et al., 2007; Izvolsky et al., 2008).

NIH-PA Author Manuscript

NIH-PA Author Manuscript

NIH-PA Author Manuscript

The secreted endosulfatase enzyme Sulfatase-1 (SULF1) cleaves HS 6-*O* sulfation and modulates BMP and FGF signaling pathways during development (Lamanna et al., 2008; Pownall et al., 2010). Loss of *Sulf1* expression by siRNA silencing in human chondrocytes impaired BMP-induced SMAD1 phosphorylation but enhanced FGF2-induced ERK1/2 phosphorylation (Otsuki et al., 2010; Pownall et al., 2010). Embryonic fibroblasts derived from $Sulf1^{-/-}$ mice are 5-fold more sensitive to FGF2 signaling as determined by ERK1/2 phosphorylation (Lamanna et al., 2008).

We previously showed that there is an increase in highly sulfated HS in the E18 male UGS relative to the female UGS, and this correlated with decreased *Sulf1* expression (Buresh et al., 2010). Ectopic *Sulf1* expression also impaired UGS bud development and FGF signaling indicating that SULF1 acts as an inhibitory factor during prostate development. However, our previous study did not address the spatial regulation of HS sulfation during prostate development or the potential regulation of *Sulf1* by other inhibitory prostate developmental signaling pathways. For the current study, the mRNA expression patterns for *Sulf1* and other HS 6-*O* modifying enzymes were examined during the initial stages of prostate morphogenesis. Of particular interest, *Sulf1* and *Hs6st1* were found to have overlapping but distinct expression patterns leading to relatively high HS 6-*O* sulfation in elongating epithelial buds. Additional studies identified a role for BMP4 and BMP7 as inducers of *Sulf1* expression in the UGS. BMP-induced *Sulf1* expression reduced epithelial HS 6-*O* sulfation and reduced ERK1/2 activation in response to FGF10. Collectively, these data indicated that BMPs limit FGF10 action in the UGS at least in part by inducing *Sulf1*. This represents a novel mechanism for coordinating the opposing actions of the FGF and BMP paracrine signaling pathways during prostate morphogenesis.

Results

Expression heparan sulfate 6-O sulfation modifying enzymes during early prostate development

The expression patterns of the HS 6-*O* sulfation modifying enzymes were determined during early prostate development using *in situ* hybridization on E17 UGS tissues. *Sulf1* expression was localized to an outer region of the UGM defined as the muscularis propria that was separated from the UGE by a *Sulf1* non-expressing region of the UGM referred to as the lamina propria (Fig. 1A, B) (Abler et al., 2011b). *Sulf1* was also expressed in the peri-mesenchymal epithelium of the E17 male and female UGS (Fig. 1A, B), but was excluded from the prostatic buds (arrows in A). *Sulf2* expression was limited to the muscularis propria and to the ventral muscularis mucosa of the male UGS (Fig. 1D). In the female UGS, *Sulf2* expression was also present in the muscularis propria and in the musclaris mucosa in the regions adjacent to the lower vagina (Fig. 1E, arrow). Expression of *Hs6st1* was present in the epithelium of E17 male and female UGSs, including the developing prostatic buds of the male UGS (Fig. 1G, arrow). *Hs6st2* was expressed in muscularis propria of the male and female UGS, in the lamina propria of the female UGS (Fig. 1J, K), and in the basal epithelium of the developing prostatic bud of the male UGS (Fig. 1J, arrow). *Hs6st3* transcripts were not detected in the UGS by RT-PCR and were subsequently not examined by *in situ* hybridization.

The expression patterns of the HS 6-*O* sulfation modifying enzymes suggested that distinct but overlapping patterns of *Sulf1* and *Hs6st1* expression may be critical determinants of 6-*O* sulfation and growth factor action at the tips of elongating prostatic buds. To further clarify this possibility, the expression patterns of *Sulf1* and *Hs6st1* were examined at additional stages of prostate development. *Sulf1* expression was dynamic and included expression in the muscularis propria during fetal development (Fig. 2A, C, D) that transitioned to expression in the peri-ductal stroma postnatally (Fig. 2F, G, H). Additional *Sulf1* expression

NIH-PA Author Manuscript

NIH-PA Author Manuscript

NIH-PA Author Manuscript

was observed in the peri-mesenchymal epithelium of the UGS and proximal prostatic ducts (Fig. 2C, D, E, G). However, *Sulf1* was not expressed in the tips of developing epithelial buds of the E18 male UGS (Fig. 2C, D) or in the distal epithelial ducts during postnatal prostate development (Fig. 2F-H). During both prenatal and postnatal prostate development, *Hs6st1* was strongly expressed throughout the epithelium of the UGS (Fig. 1E) and the epithelium of developing prostatic ducts (Fig. 3). Lower-level expression of *Hs6st1* was also present in the peri-epithelial stroma of the prostate (examples indicated by arrowheads in Fig. 3D).

Highly-sulfated heparan sulfate localizes to the prostatic epithelial buds of the developing UGS

The presence of *Hs6st1* and absence *Sulf1* expression at the tips of developing prostatic buds predicted relatively robust 6-*O* sulfated HS at the bud tips. Antibodies directed against HS domains with specific sulfation patterns have previously been developed using phage-display techniques and have been used to detect HS in a variety of tissues including the kidney and testes (van Kuppevelt et al., 1998; Dennissen et al., 2002). The HS specific antibody, RB4CD12, generated by this method has been shown bind specifically to tri-sulfated HS oligosaccharides (containing 2-*O*, 6-*O*, and *N*-sulfation) but cannot bind HS that has been 6-*O* desulfated by SULF1 (Hossain et al., 2010). In the E18 male UGS, the RB4CD12 antibody fragment localized highly sulfated HS to the UGE with particularly robust staining in the developing prostatic epithelial buds (arrows in Fig. 4A and B). The specificity of the antibody for HS was confirmed by the absence of staining in E18 male UGS tissues that were pretreated with heparinase (Fig. 4C).

BMP4 and BMP7 induce Sulf1 expression in the UGS

The epithelial *Sulf1* mRNA expression pattern appeared to match predicted sites of BMP4 and BMP7 signaling in the UGS and developing prostate suggesting possible regulation of SULF1 by BMPs. To test this possibility, UGSs were cultured in the presence of BMP4 or BMP7, and these treatments resulted in a 2-fold and 4-fold increase in *Sulf1* expression, respectively (Fig. 5A). Further analysis of BMP-treated UGS tissues by *in situ* hybridization indicated that increased *Sulf1* expression could be attributed to an increase in the number of peri-mesenchymal epithelial cells that expressed *Sulf1* (Fig. 5B-D).

BMPs modulate epithelial HS sulfation in the UGS

The induction of *Sulf1* expression by BMP4 and BMP7 in cultured UGS tissues suggested that HS 6-*O* sulfation would be reduced by BMP treatments. To test this possibility, immunofluorescent staining with the RB4CD12 antibody was performed on male UGS tissues that were cultured for 48 hours with BMP4 or BMP7. Staining for tri-sulfated HS was decreased in the epithelium of UGSs cultured with either BMP4 or BMP7 (Fig. 6B and C, respectively) compared with control cultured UGS tissues (Fig. 6A). This confirmed that BMP-induced *Sulf1* expression resulted in reduced tri-sulfated HS in the UGS.

BMP-induced Sulf1 expression impairs FGF10-induced ERK1/2 phosphorylation

FGF10 signaling promotes growth and branching of the UGS via the activation and phosphorylation of mitogen-activated protein kinases ERK1 and ERK2 (Kuslak and Marker, 2007), and tri-sulfated HS promotes signaling by FGF10 through interactions with the ligand-receptor complex (Makarenkova et al., 2009). This suggested BMP induced *Sulf1* expression might impair FGF signaling through modifications to HS sulfation. E15 UGS tissues were cultured with exogenous BMP4 or BMP7 for 48 hours and then stimulated with FGF10. FGF10 induced ERK1/2 phosphorylation in the epithelium of control UGS tissues

NIH-PA Author Manuscript

NIH-PA Author Manuscript

NIH-PA Author Manuscript

(Fig. 7A, D) but phosphorylation of ERK1/2 was impaired in the epithelium of BMP-treated UGS tissues (Fig. 7B, C, E-G).

Discussion

The regulation of HS sulfation is an important determinant of developmental growth factor signaling in many organ systems. Of particular importance is the regulation of 6-*O* sulfation by the intracellular sulfotransferases, *Hs6st1, Hs6st2*, and *Hs6st3* as well as the extracellular sulfatases, *Sulf1* and *Sulf2*. Each of these sulfation-modifying enzymes has a unique developmental expression pattern that contributes to overall spatial and temporal regulation of 6-*O* sulfation. Multiple studies have shown that these enzymes are critical for normal development in both vertebrates and invertebrates (Habuchi et al., 2007; Danesin et al., 2006; Kleinschmit et al., 2010), and our previous study implicated down-regulation of *Sulf1* as an important feature of prostate development (Buresh et al., 2010).

The development of the prostate occurs through branching morphogenesis that is regulated by complex crosstalk among paracrine growth factor signaling pathways (Prins and Putz, 2008; Marker et al., 2003). Each step of branching morphogenesis including epithelial bud development, ductal elongation, and branch point formation are temporally and spatially regulated by growth factors that individually promote or impair epithelial morphogenesis. Signaling events occurring at the interface between the developing prostatic epithelium and mesenchyme/stroma are viewed as particularly critical because many epithelial-expressed growth factors bind mesenchymal receptors while many mesenchymal-expressed growth factors bind epithelial receptors. In the present study, we sought to identify how spatial and temporal regulation of HS 6-*O* modifying enzymes might contribute to the regulation of growth factor signaling during prostate development. *Hs6st1, Hs6st2*, *Sulf1* and *Sulf2* were each expressed during prostate development in distinct patterns (Figs. 1-3). Notably, *Hs6st1* was expressed throughout the epithelium of developing prostate from the bud stage onward while *Sulf1* expression was present in the epithelium except at the tips of prostatic buds and ducts. This predicted the enhanced presence of highly sulfated HS in the developing prostatic buds/ductal tips, and this was confirmed by immunostaining with the RB4CD12 antibody that localized highly sulfated HS to the epithelium of the E18 male UGS with strong staining in the epithelial prostatic buds (Fig 4).

Higher levels of highly sulfated HS at the tips of prostatic buds/ducts likely enhances FGF signaling at the ductal tips. Both FGF7 and FGF10 are expressed in the UGS during prostatic epithelial bud development and ductal morphogenesis, but $Fgf7^{-/-}$ UGSs develop into normal prostates while $Fgf10c^{-/-}$ UGSs fail to form prostates (Donjacour et al., 2003). Both FGF7 and FGF10 bind epithelial FGFR2IIIb to promote epithelial proliferation (Kuslak et al., 2007), but Mohammadi and colleagues have shown the interaction between FGF10 and FGFR2IIIb requires 6-*O* sulfated HS, which is not necessary for FGF7 ligand-receptor binding (Yeh et al., 2003). The modulation of HS sulfation in the UGS likely contributes to the differential roles of FGF10 and FGF7 during ductal morphogenesis, and our data suggests *Hs6st1* and *Sulf1* modulation of HS likely contributes to this effect. The present study also further clarified the relationship among BMP signaling, *Sulf1* action, and FGF signaling during prostate development. *Bmp4*, *Bmp7*, and *Sulf1* all act as inhibitors of prostate morphogenesis (Grishina et al., 2005; Lamm et al., 2001; Buresh et al., 2010). The expression pattern of *Sulf1* in the UGS/prostate epithelium also matched predicted sites of BMP signaling. Both BMP4 and BMP7 induced *Sulf1* expression in the UGS epithelium (Fig. 5). This correlated with reduced HS sulfation (Fig. 6) and impaired activation of the ERK1/2 mitogen activated kinases in response to FGF10 stimulation (Fig. 7). Collectively, these data suggest a model for prostate development in which BMP signaling contributes to

NIH-PA Author Manuscript

NIH-PA Author Manuscript

NIH-PA Author Manuscript

the spatial patterning of prostate epithelial bud formation and ductal outgrowth by limiting FGF10 signaling, at least in part, through induction of *Sulf1* expression.

Experimental Procedures

Experimental Animals

Female CD1 mice (Charles River Laboratories) were obtained as timed pregnant animals and sacrificed in the morning 15, 16, or 18 days after being bred and C57BL6 mice were obtained 17 days after being bred. UGSs were dissected out of female and male embryos as previously described (Staack et al., 2003). C57BL6 tissues were used for the in situ hybridization experiments in Fig. 1 while the experiments in Figs. 2-7 were performed using CD1 mouse tissues. All animal experimentation in this study was conducted in accord with accepted standards of humane animal care as outlined in the NIH Guide for the Care and Use of Laboratory Animals, and the experimentation was approved by the Animal Care and Use Committee of the University of Wisconsin-Madison.

In vitro organ cultures

UGSs were dissected out of mice and cultured at 5% CO_2, 37°C at the air/medium interface as previously described (Buresh et al., 2010). Basal medium was supplemented as indicated in the figure legends and sometimes included 10^{-8} M testosterone, 300 ng/mL human BMP4, 300 ng/mL human BMP7, and 2.5 μg/mL human FGF10. All recombinant proteins used in this study were obtained from Peprotech, Inc. Culture medium was changed every 24 hours during culture. For experiments with FGF10 stimulation, tissues were cultured with BMP growth factors but without FGF10 for 48 hours, and then media was replaced with basal medium containing BMP growth factors and FGF10. Tissues were then cultured for 20 minutes at 37°C, 5% CO_2. Tissues were immediately processed for RNA or immunochemistry.

RNA isolation, reverse transcriptase PCR and quantitative real time PCR

Pools of 3-4 UGSs were combined following UGS culture, homogenized with pestle, and processed with the Nucleospin RNA II kit (McHerey-Nagel) with DNase digest per the manufacturer's protocol. Reverse transcription was completed using 1 μg RNA and the Superscript II (Invitrogen) reagents as previously described (Buresh et al., 2010). Real-time PCR was completed using the OneStepPlus PCR system (Applied Biosystems, Inc.) and Power Sybr Green Mix (Applied Biosystems, Inc.) with 5 μl of cDNA from the reverse transcriptase reaction. Relative mRNA expression levels were calculated as described previously (Wong and Medrano, 2005). Primer sequences were as follows: *mSulf1* F: TGC TCA CTG GGA AGT ACG TG and R: AGG GAT GTA GCT GCC ATT GT. Transcript levels were normalized to *m18S*; primer sequences were F: GCC GCT AGA GGT GAA ATT CTT G and R: CAT TCT TGG CAA ATG CTT TCG.

Western Blotting

Protein was obtained from pools of 3-4 UGS tissues following culture. Tissues were lysed by sonication in modified RIPAS buffer (50 mM Tris-HCl, 1% Nonidot-P40, 0.25% sodium deoxycholate, 150 mM NaCl, 1 mM EDTA, 10 mM NaF) with protease inhibitor cocktail (Roche). 5-μg of protein was run on a 10% polyacrylamide gel and transferred to a PVDF membrane (GE Healthcare). Protein was detected with the Amersham chemiluminescent reagent (GE Healthcare) on the Storm imager. Antibodies for phospho-MAPK42/44 (1:2000; #4376), and total-MAPK42/P44 (1:2000; #9102) were obtained from Cell Signaling Technology.

NIH-PA Author Manuscript

NIH-PA Author Manuscript

NIH-PA Author Manuscript

In situ Hybridization and Riboprobe Synthesis

Primers used to amplify the *Sulf1, Sulf2, Hs6st1, and Hs6st2* mRNA transcripts from pooled adult mouse prostate and E16 male and female mouse embryo cDNA contained either T7 (antisense) or SP6 (sense) polymerase sequences. Primer sequences were as follows: *Sulf1*, CGC ATA CGA TTT AGG TGA CAC TAT AGA CAT CCG TGT GCCTTT CTT C and CGA TGT TAA TAC GAC TCA CTA TAG GGT TGG TGT TCC CTT GTT CCT C; *Sulf2*, CGC ATA CGA TTT AGG TGA CAC TAT AGA CTG GAT ATC GCT GGA CTG G and CGA TGT TAA TAC GAC TCA CTA TAG GGT GTG CAG CAG CTT GTG GTC TTT C; *Hs6st1*, CGC ATA CGA TTT AGG TGA CAC TAT AGG CTT TCA AGG TCA GGG TCA G and CGA TGT TAA TAC GAC TCA CTA TAG GGT CAC AGG TCT GCT GGA AAT G; *Hs6st2*, CGC ATA CGA TTT AGG TGA CAC TAT AGT TCG CAT GCT ATC TGA CCT G and CGA TGT TAA TAC GAC TCA CTA TAG GGA GGA AGC AGG ATG TGT TTG G. cDNA templates were amplified by standard PCR techniques (Abler et al., 2011b). Antisense and sense digoxigenin (DIG)-labeled probes were transcribed with their respective polymerases and DIG-labeled nucleotide mixture (Roche Applied Science) and subsequently purified using the Nucleospin RNA II kit (McHerey-Nagel) with DNase digest per the manufacturer's protocol. Probe sequences were confirmed by sequencing analysis and final DIG-riboprobe purity was confirmed by gel electrophoresis.

Embryo UGS tissues from E17 C57BL6 mice were sectioned at 50-μm thickness (Fig. 1) and processed using the whole mount *in situ* hybridization (ISH) procedure previously reported (Abler et al., 2011b). For thin-section ISH, E16 and E18 UGS tissues were obtained from CD1 mice and prostate tissues were obtained from postnatal day 1, 3 or 14 CD1 mouse pups (Figs. 2, 3, and 5). Immediately following dissection or culture, UGS tissues were embedded in OCT compound and flash frozen. Tissues were cryosectioned at 10-μm thickness and immediately fixed in 4% paraformaldehyde in PBS (pH 7.4) for 1 hour. Tissues were further digested with Proteinase-K and quenched with 6% H_2O_2 in PBS. Tissues were hybridized with DIG-labeled probes at 61°C overnight, rinsed extensively, and localized with an alkaline phosphotase conjugated anti-DIG antibody (Roche). Tissues were developed with BM Purple AP substrate (Roche) for 1-2 days before being mounted and imaged.

Immunohistochemistry and Immunofluorescence

Following culture, UGSs were immediately embedded in O.C.T. medium and flash frozen. Tissues were cryosectioned at 8-μm thickness, fixed in 4% paraformaldehyde in PBS for 30 minutes and quenched with 3% hydrogen peroxide solution for 10 minutes. For phospho-ERK staining, slides were blocked with 5% goat serum and incubated with 1:200 dilution of anti-phospho-MAPK42/44 (Cell Signaling Technology #4376) in blocking solution overnight. Following a series of washes, slides were incubated with secondary biotinylated anti-rabbit antibody for one hour. Slides were washed, incubated with the Vectastain ABC kit (Vector Laboratories), washed again, and stained using peroxidase substrate kit DAB (Vector Laboratories). Finally slides were counterstained with hematoxylin, dehydrated, and mounted.

For immunofluorescence with anti-HS antibody, tissues were blocked in 3% BSA in PBS for one hour and then overnight with the RB4CD12 antibody (1:10 dilution of periplasmic fraction, Myc-tagged V_H fragment) in 3% BSA in PBS (Hossain et al., 2010). Following a series of washes, slides were incubated with 1:1000 dilution of AlexaFluor-647 anti-Myc antibody (Cell Signaling Technology #2233) in 2.5% Sheep Serum/3% BSA/PBS. Slides were washed and mounted with Vectashield hard-set mounting media with DAPI (Vector Labs). Slides were imaged by confocal microscopy on the Olympus BX61 microscope

NIH-PA Author Manuscript

NIH-PA Author Manuscript

NIH-PA Author Manuscript

equipped with the Fluoview1000 confocal imaging system and the Olympus Fluoview v1.7b software package.

Statistical Analyses

Statistics were evaluated by ANOVA analysis with Bonferroni post hoc correction using the Prism v5.0b software program.

Acknowledgments

This manuscript was supported by grants to PCM: Grant sponsor: NIDDK, grant number DK091193 (formerly AG024278); Grant sponsor: NCI, grant number CA140217 and to CMV grant sponsor NIDDK, grant number DK083425.

References

Abler LL, Keil KP, Mehta V, Joshi PS, Schmitz CT, Vezina CM. A high-resolution molecular atlas of the fetal mouse lower urogenital tract. Dev Dyn. 2011a; 240:2364–2377. [PubMed: 21905163]

Abler LL, Mehta V, Keil KP, Joshi PS, Flucus CL, Hardin HA, Schmitz CT, Vezina CM. A high throughput in situ hybridization method to characterize mRNA expression patterns in the fetal mouse lower urogenital tract. J Vis Exp. 2011b; 54:e2912.

Buresh RA, Kuslak SL, Rusch MA, Vezina CM, Selleck SB, Marker PC. Sulfatase 1 Is an Inhibitor of Ductal Morphogenesis with Sexually Dimorphic Expression in the Urogenital Sinus. Endocrinology. 2010; 151:3420–3431. [PubMed: 20410206]

Cook C, Vezina CM, Allgeier SH, Shaw A, Yu M, Peterson RE, Bushman W. Noggin is required for normal lobe patterning and ductal budding in the mouse prostate. Dev Biol. 2007; 312:217–230. [PubMed: 18028901]

Danesin C, Agius E, Escalas N, Ai X, Emerson C, Cochard P, Soula C. Ventral neural progenitors switch toward an oligodendroglial fate in response to increased Sonic hedgehog (Shh) activity: Involvement of sulfatase 1 in modulating Shh signaling in the ventral spinal cord. J Neurosci. 2006; 26:5037–5048. [PubMed: 16687495]

Dennissen MABA, Jenniskens GJ, Pieffers M, Versteeg EMM, Petitou M, Veerkamp JH, van Kuppevelt TH. Large, tissue-regulated domain diversity of heparan sulfates demonstrated by phage display antibodies. J Biol Chem. 2002; 277:10982–10986. [PubMed: 11790764]

Donjacour AA, Thomson AA, Cunha GR. FGF-10 plays an essential role in the growth of the fetal prostate. Dev Biol. 2003; 261:39–54. [PubMed: 12941620]

Esko JD, Lindahl U. Molecular diversity of heparan sulfate. J Clin Invest. 2001; 108:169–173. [PubMed: 11457867]

Grishina IB, Kim SY, Ferrara C, Makarenkova HP, Walden PD. BMP7 inhibits branching morphogenesis in the prostate gland and interferes with Notch signaling. Dev Biol. 2005; 288:334–347. [PubMed: 16324690]

Habuchi H, Miyake G, Nogami K, Kuroiwa A, Matsuda Y, Kusche-Gullberg M, Habuchi O, Tanaka M, Kimata K. Biosynthesis of heparan sulphate with diverse structures and functions: two alternatively spliced forms of human heparan sulphate 6-O-sulphotransferase-2 having different expression patterns and properties. Biochem J. 2003; 371:131–142. [PubMed: 12492399]

Habuchi H, Nagai N, Sugaya N, Atsumi F, Stevens RL, Kimata K. Mice deficient in heparan sulfate 6-O-sulfotransferase-1 exhibit defective heparan sulfate biosynthesis, abnormal placentation, and late embryonic lethality. J Biol Chem. 2007; 282:15578–15588. [PubMed: 17405882]

Habuchi H, Tanaka M, Habuchi O, Yoshida K, Suzuki H, Ban K, Kimata K. The occurrence of three isoforms of heparan sulfate 6-O-sulfotransferase having different specificities for hexuronic acid adjacent to the targeted N-sulfoglucosamine. J Biol Chem. 2000; 275:2859–2868. [PubMed: 10644753]

Hossain MM, Hosono-Fukao T, Tang R, Sugaya N, van Kuppevelt TH, Jenniskens GJ, Kimata K, Rosen SD, Uchimura K. Direct detection of HSulf-1 and HSulf-2 activities on extracellular

NIH-PA Author Manuscript

NIH-PA Author Manuscript

NIH-PA Author Manuscript

heparan sulfate and their inhibition by PI-88. Glycobiology. 2010; 20:175–186. [PubMed: 19822709]

Huang L, Pu Y, Alam S, Birch L, Prins GS. The role of Fgf10 signaling in branching morphogenesis and gene expression of the rat prostate gland: lobe-specific suppression by neonatal estrogens. Dev Biol. 2005; 278:396–414. [PubMed: 15680359]

Izvolsky KI, Lu J, Martin G, Albrecht KH, Cardoso WV. Systemic inactivation of Hs6st1 in mice is associated with late postnatal mortality without major defects in organogenesis. Genesis. 2008; 46:8–18. [PubMed: 18196599]

Kleinschmit A, Koyama T, Dejima K, Hayashi Y, Kamimura K, Nakato H. Drosophila heparan sulfate 6-O endosulfatase regulates Wingless morphogen gradient formation. Dev Biol. 2010; 345:204–214. [PubMed: 20637191]

Kuslak SL, Marker PC. Fibroblast growth factor receptor signaling through MEK-ERK is required for prostate bud induction. Differentiation. 2007; 75:638–651. [PubMed: 17309601]

Kuslak SL, Thielen JL, Marker PC. The mouse seminal vesicle shape mutation is allelic with Fgfr2. Development. 2007; 134:557–565. [PubMed: 17202188]

Lamanna WC, Frese MA, Balleininger M, Dierks T. Sulf loss influences N-, 2-o-, and 6-o-sulfation of multiple heparan sulfate proteoglycans and modulates fibroblast growth factor signaling. J Biol Chem. 2008; 283:27724–27735. [PubMed: 18687675]

Lamm ML, Podlasek CA, Barnett DH, Lee J, Clemens JQ, Hebner CM, Bushman W. Mesenchymal factor bone morphogenetic protein 4 restricts ductal budding and branching morphogenesis in the developing prostate. Dev Biol. 2001; 232:301–314. [PubMed: 11401393]

Lin YS, Liu GQ, Zhang YY, Hu YP, Yu K, Lin CH, McKeehan K, Xuan JW, Ornitz DM, Shen MM, Greenberg N, McKeehan WL, Wang F. Fibroblast growth factor receptor 2 tyrosine kinase is required for prostatic morphogenesis and the acquisition of strict androgen dependency for adult tissue homeostasis. Development. 2007; 134:723–734. [PubMed: 17215304]

Makarenkova HP, Hoffman MP, Beenken A, Eliseenkova AV, Meech R, Tsau C, Patel VN, Lang RA, Mohammadi M. Differential interactions of FGFs with heparan sulfate control gradient formation and branching morphogenesis. Sci Signal. 2009; 2:ra55. [PubMed: 19755711]

Marker PC, Donjacour AA, Dahiya R, Cunha GR. Hormonal, cellular, and molecular control of prostatic development. Dev Biol. 2003; 253:165–174. [PubMed: 12645922]

Otsuki S, Hanson SR, Miyaki S, Grogan SP, Kinoshita M, Asahara H, Wong CH, Lotz MK. Extracellular sulfatases support cartilage homeostasis by regulating BMP and FGF signaling pathways. Proceed Nat Acad Sci USA. 2010; 107:10202–10207.

Pownall ME, Guiral EC, Faas L. Neural crest migration requires the activity of the extracellular sulphatases XtSulf1 and XtSulf2. Dev Biol. 2010; 341:375–388. [PubMed: 20206618]

Prins GS, Huang L, Birch L, Pu Y. The role of estrogens in normal and abnormal development of the prostate gland. Ann N Y Acad Sci. 2006; 1089:1–13. [PubMed: 17261752]

Prins GS, Putz O. Molecular signaling pathways that regulate prostate gland development. Differentiation. 2008; 76:641–659. [PubMed: 18462433]

Ratzka A, Mundlos S, Vortkamp A. Expression Patterns of Sulfatase Genes in the Developing Mouse Embryo. Dev Dyn. 2010; 239:1779–1788. [PubMed: 20503373]

Staack A, Donjacour AA, Brody J, Cunha GR, Carroll P. Mouse urogenital development: a practical approach. Differentiation. 2003; 71:402–413. [PubMed: 12969333]

Thomson AA, Cunha GR. Prostatic growth and development are regulated by FGF10. Development. 1999; 126:3693–3701. [PubMed: 10409514]

van Kuppevelt TH, Dennissen MABA, van Venrooij WJ, Hoet RMA, Veerkamp JH. Generation and application of type-specific anti-heparan sulfate antibodies using phage display technology - Further evidence for heparan sulfate heterogeneity in the kidney. J Biol Chem. 1998; 273:12960–12966. [PubMed: 9582329]

Viviano BL, Paine-Saunders S, Gasiunas N, Gallagher J, Saunders S. Domain-specific modification of heparan sulfate by Qsulf1 modulates the binding of the bone morphogenetic protein antagonist noggin. J Biol Chem. 2004; 279:5604–5611. [PubMed: 14645250]

Wong ML, Medrano JF. Real-time PCR for mRNA quantitation. Biotechniques. 2005; 39:75–85. [PubMed: 16060372]

NIH-PA Author Manuscript

NIH-PA Author Manuscript

NIH-PA Author Manuscript

Yeh BK, Igarashi M, Eliseenkova AV, Plotnikov AN, Sher I, Ron D, Aaronson SA, Mohammadi M. Structural basis by which alternative splicing confers specificity in fibroblast growth factor receptors. Proceed Nat Acad Sci USA. 2003; 100:2266–2271.

Zhang YY, Zhang J, Lin YS, Lan YS, Lin CH, Xuan JW, Shen MM, McKeehan WL, Greenberg NM, Wang F. Role of epithelial cell fibroblast growth factor receptor substrate 2 alpha in prostate development, regeneration and tumorigenesis. Development. 2008; 135:775–784. [PubMed: 18184727]

Zhao W, Sala-Newby GB, Dhoot GK. Sulf1 expression pattern and its role in cartilage and joint development. Dev Dyn. 2006; 235:3327–3335. [PubMed: 17061267]

NIH-PA Author Manuscript

NIH-PA Author Manuscript

NIH-PA Author Manuscript

Bullet points

- Heparan Sulfate sulfation modifying enzymes *Sulf1* and *Hs6st1* have distinct but overlapping expression domains in the developing prostate
- BMP4 and BMP7 induced *Sulf1* expression in the developing prostate and decreased epithelial HS 6-*O* sulfation
- BMP4 and BMP7 reduced ERK1/2 activation in response to FGF10

NIH-PA Author Manuscript
NIH-PA Author Manuscript
NIH-PA Author Manuscript

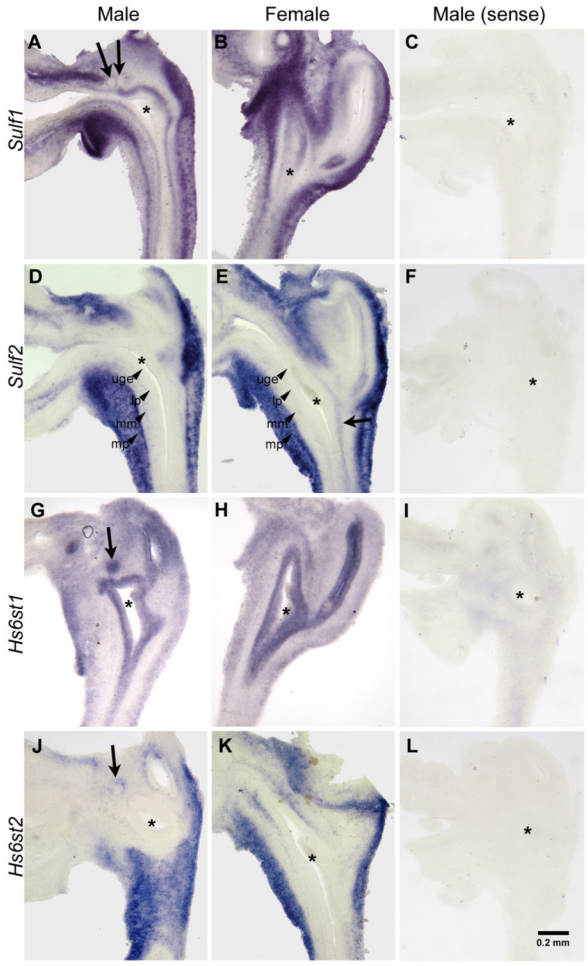

Figure 1. Expression of HS 6-*O*sulfation modifying enzymes during early prostate development

In situ hybridization was used to localize *Sulf1* in male (A) and female (B), *Sulf2* in male (D) and female (E), *Hs6st1* in male (G) and female (H), and *Hs6st2* in male (J) and female (K) e17 UGSs. *Sulf1* was expressed in the muscularis propria and UGE immediately adjacent to the UGM but not in prostatic epithelial buds (arrows in A). *Sulf2* was expressed was in the muscularis propria and musclaris mucosa adjacent to the lower vagina (arrow in E). *Hs6st1* was expressed throughout the epithelium including prostatic epithelial buds (arrow in G). *Hs6st2* was expressed in the muscularis propria, in a thin layer of peri-urethral mesenchyme adjacent to the epithelium, and in the lamina propria surrounding the developing prostatic epithelial buds (arrow in J). Sense riboprobes were used as negative controls to confirm the specificity of staining for *Sulf1* (C), *Sulf2* (F), *Hs6st1* (I), and *Hs6st2* (L). The UGE, lamina propria (lp), muscularis mucosa (mm), and muscularis propria (mp) are labeled in D and E for clarity. Asterisks indicate the approximate center of the UGS. A scale bar for all panels is shown in L.

NIH-PA Author Manuscript
NIH-PA Author Manuscript
NIH-PA Author Manuscript

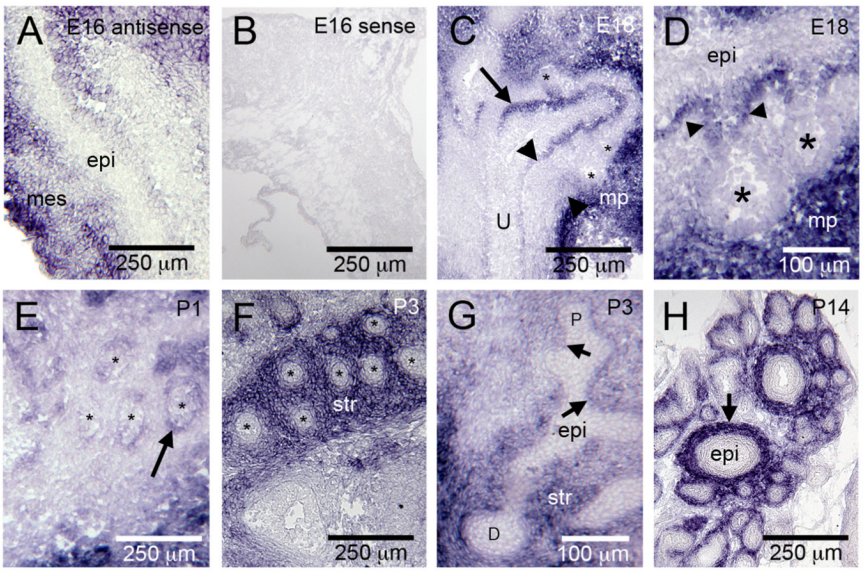

Figure 2. *Sulf1* expression is dynamically regulated during prostate development

Sulf1 transcripts were detected in the developing mesenchyme (mes) but not the epithelium (epi) at E16 (A). A *Sulf1* sense probe was used as a negative control (B). At E18, *Sulf1* transcripts were detected in the muscularis propria (mp in C and D), and in the peri-mesenchymal epithelium (C, arrow). Expression was not detected in the tips of developing prostatic buds (indicated by *) or in the peri-epithelial mesenchyme (C, arrowhead). A high magnification view (D), shows *Sulf1* expression was detected in the most proximal region of the epithelial buds (arrowheads) but not in the bud tips (indicated by *). At P1, *Sulf1* expression was localized to the peri-mesenchymal epithelium of the proximal ducts (E arrow; * indicate epithelial ducts). At P3, *Sulf1* was expressed in the distal stroma (str) but not in the distal epithelium (F; * indicate epithelial ducts). A longitudinal section through a P3 duct (G) further illustrates the pattern of *Sulf1* expression (str, stroma; arrows indicate branch points; P, proximal; D, distal). At P14, *Sulf1* expression was restricted to the stroma (H, arrow) surrounding epithelial ducts.

NIH-PA Author Manuscript
NIH-PA Author Manuscript
NIH-PA Author Manuscript

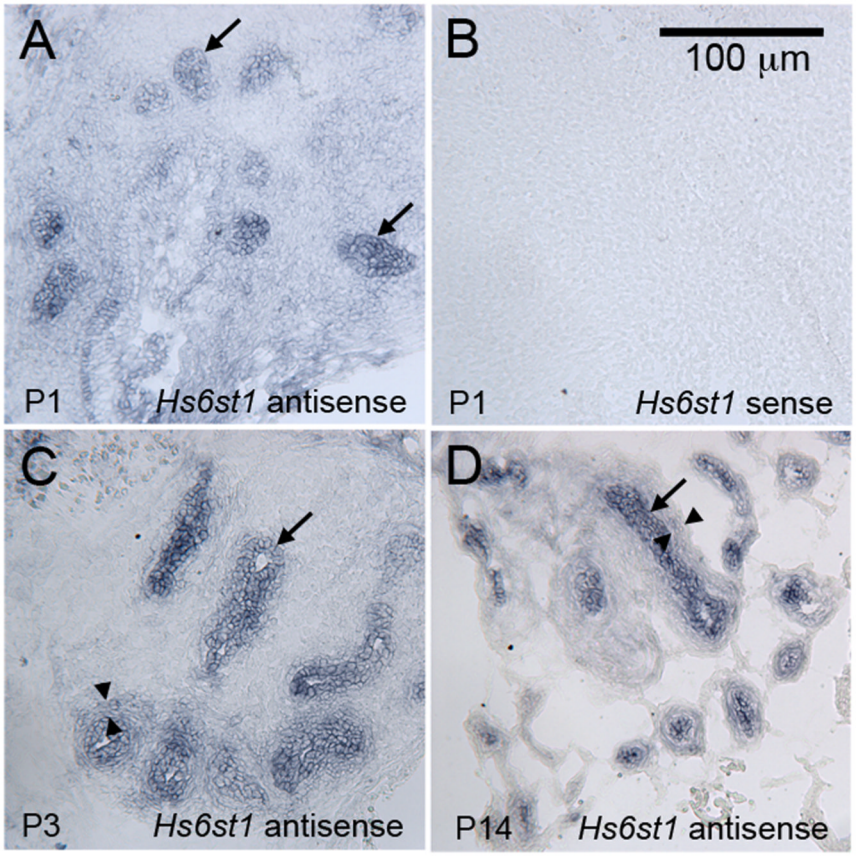

Figure 3. *Hs6st1* is expressed in the epithelium of the developing prostate

Antisense riboprobes complementary to the *Hs6st1* mRNA detected strong expression in throughout the developing epithelial ducts at P1 (A), P3 (C), and P14 (D). An *Hs6st1* sense probe was used as a negative control, and it did not stain developing prostatic tissues (P1 shown as example in B). Lower expression that was above the background staining of the sense probe was also observed in the peri-epithelial mesenchyme (examples indicated between the arrowheads in C and D). A scale bar for all panels is shown in B.

NIH-PA Author Manuscript
NIH-PA Author Manuscript
NIH-PA Author Manuscript

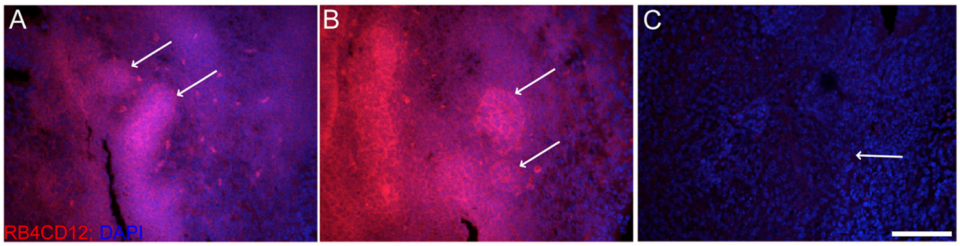

Figure 4. RB4CD12 staining localizes tri-sulfated HS to developing epithelial buds in the UGS

The RB4CD12 antibody fragment was used to localize the tri-sulfated HS epitope (containing 2-*O*, 6-*O*, and *N*-sulfation) in the E18 UGS male UGS. (A and B). Highly tri-sulfated HS (red) was localized to the epithelium of the male UGS during bud development, and staining was most intense in developing epithelial buds (arrows in A and B). As a negative control, E18 male UGS tissues were pre-treated with heparinase to cleave HS (C). Heparinase treated sections did not bind the RB4CD12 antibody, confirming the HS-specificity of RB4CD12 staining in the UGS (arrow in C indicates epithelial-mesenchymal boundary). All images were counterstained with DAPI nuclear stain (blue) and imaged at 20× magnification with confocal microscopy. Scale bar in C indicates 100 μm scale for A-C.

NIH-PA Author Manuscript

NIH-PA Author Manuscript

NIH-PA Author Manuscript

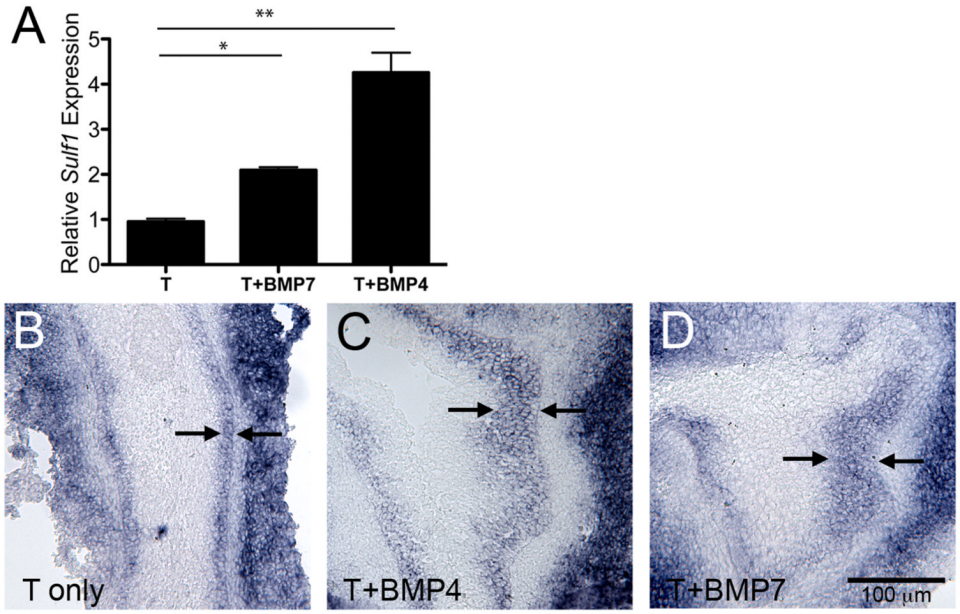

Figure 5. BMP4 and BMP7 induce *Sulf1* expression

E15 male UGS tissues were cultured with 10^{-8}M testosterone (T) with or without the addition of 300 ng/mL BMP7 or 300 ng/mL BMP4 for 48 hours. *Sulf1* mRNA relative expression was determined by real-time RT-PCR and was normalized to *18S* mRNA expression (A). Graphs depict the average fold-change (± SEM) in expression relative to controls for a representative experiment (n=3 per group). Statistically significant increases in *Sulf1* expression in response to BMP treatments were observed in four independent experiments (A, and data not shown). Statistical significance was determined by ANOVA with Bonferroni post-hoc analysis (*:$P<0.01$, **:$P<0.0001$). Spatial expression of *Sulf1* mRNA was determined in serial sections of UGS tissues cultured in the presence of testosterone only (B) or with testosterone and BMP4 (C) or testosterone and BMP7 (D). Representative images show epithelial *Sulf1* expression was restricted to a narrow band of peri-mesenchymal cells approximately three cell layers thick in testosterone only control tissues, and was expressed in a thicker band of peri-mesenchymal epithelial cell layers (arrows indicate *Sulf1* expressing epithelial cells in each panel) in BMP treated UGS tissues. A scale bar for B-D is shown in D.

NIH-PA Author Manuscript

NIH-PA Author Manuscript

NIH-PA Author Manuscript

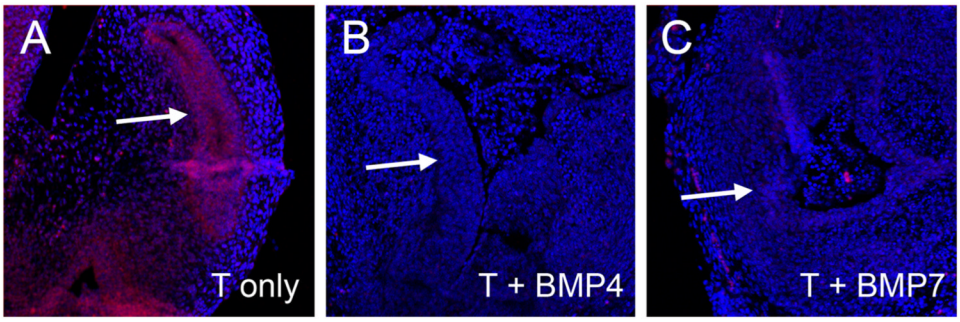

Figure 6. Heparan sulfate sulfation is reduced in BMP treated UGS tissues

E15 UGS tissues were cultured for 48 hours in the presence of testosterone only (A), testosterone + BMP4 (B), or testosterone + BMP7 (C). Tissue sections were evaluated using immunofluorescence staining with the RB4CD12 antibody to detect the tri-sulfated HS epitope (containing 2-*O*, 6-*O*, and *N*-sulfation). Significant UGE staining (red) was present in the testosterone only treatment (arrow in A) and undetectable in the UGE following BMP4 or BMP7 treatments (arrows in B and C). Tissue sections were counterstained with DAPI (blue stain in all panels).

NIH-PA Author Manuscript
NIH-PA Author Manuscript
NIH-PA Author Manuscript

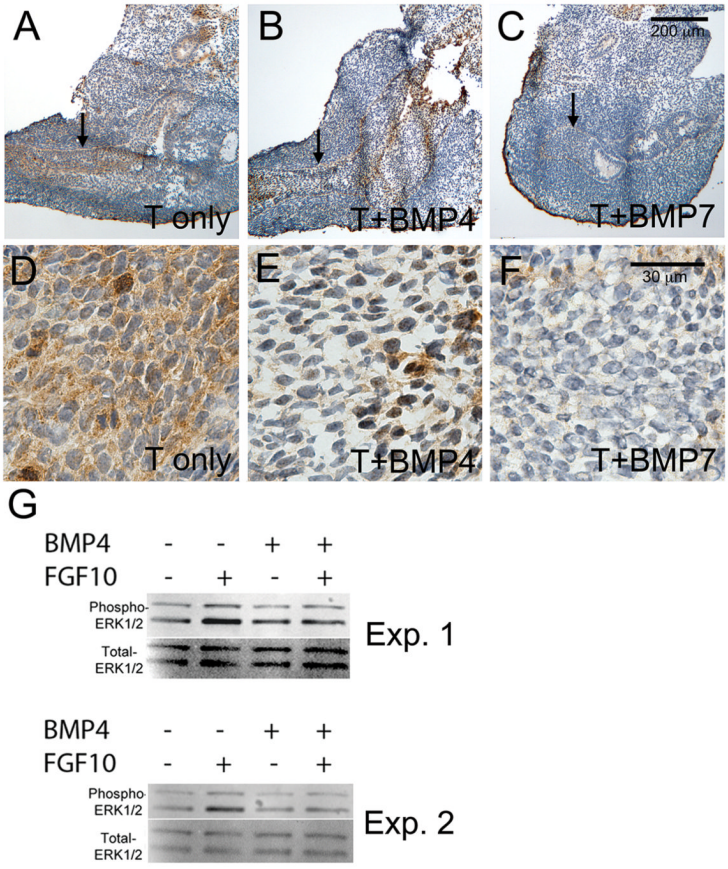

Figure 7. FGF10-induced ERK1/2 activation is reduced in BMP treated UGS tissues

E15 UGS tissues were cultured for 48 hours in the presence of testosterone only (A, D), testosterone + BMP4 (B, E), or testosterone + BMP7 (C, F). At the end of the culture period, tissues were treated with FGF10 for 20 minutes and then processed for analysis of ERK1/2 activation. Tissue sections were evaluated using immunostaining with an antibody to detect phosphorylated (activated) ERK1/2. Significant staining (brown stain) was present in the testosterone only treatment and reduced in the UGE following BMP4 or BMP7 treatments (UGE indicted by the arrows in A-C and shown at higher magnification in D-F). Overall reductions in UGS phospho-ERK1/2 were also detected by Western blotting following BMP4 treatment in four independent experiments (G and data not shown). Results from two independent experiments (Exp. 1 and Exp. 2) are shown in G. Tissue sections were counterstained with hematoxylin (purple stain in A-F). Scale bars for A-C and D-F are shown in panels C and F respectively.